

Article ID:1004-4213(2011)08-1137-6

Novel Compact Low Refractive Index Contrast Silica-on-Silicon AWG

WANG Wen-min^{1, 2}, LIU Wen¹, MA Wei-dong²

(1 Wuhan National Laboratory for Optoelectronics, College of Optoelectronic Science and Engineering,
Huazhong University of Science and Technology, Wuhan 430074, China)

(2 Accelink Technologies Co., Ltd., Wuhan 430074, China)

Abstract: Arrayed waveguide grating (AWG)-type optical components are widely used in optical transmission system, and the low cost AWG chips are in more and more urgent need. Among all the methods for lowering the AWG cost, reducing the AWG chip size is one of the most effective methods. A novel compact AWG based on low refractive index contrast silica-on-silicon (SoS) technology was proposed. In this AWG, only the segments connected with the slab waveguides in the input and output waveguides are air trench (AT) waveguides. By using these AT segments, the distance between the adjacent output waveguides connected with the output slab was decreased greatly, so the focuses of slab waveguides, and the number of arrayed waveguides were decreased greatly. Thus, the size of AWG chip was decreased dramatically. The arrayed waveguides and the segments coupling to fibers in the input or output waveguides were all fabricated with low refractive index contrast waveguides, for the purpose to obtain low coupling losses with fibers and good performances as traditional SoS AWGs. The size of an AWG designed consisting 40 channels on 100 GHz ITU grid is only 23.88 mm×10.5 mm, which area is about 1/6 of a traditional AWG with the same function.

Key words: Air trench; Arrayed waveguide grating(AWG); Passband width; Silica on silicon (SoS) technology

CLCN: TN256

Document Code: A

doi:10.3788/gzxb20114008.1137

0 Introduction

Dense wavelength division multiplexer (DWDM) based on arrayed waveguide grating (AWG) is widely used in the backbone, metropolitan, and access networks, for its advantages of low cost, preferable optical specifications, and high reliability. The most important technologies used for manufacturing the AWGs are silica-on-silicon (SoS) technology and InP-based semiconductor technology^[1]. The SoS AWGs occupy the major AWG market^[2], for they have the advantages of low propagation loss, high fiber-coupling efficiency, and mature manufacture technologies. The disadvantage of SoS AWG is that it has a relative large scale, for it is popularly manufactured with low refractive index contrast waveguides^[2]. The relative refractive index contrast of commercial SoS AWG is popularly 0.75%— Δ .

Large size of AWG chip means low production and high cost. For the purpose of fabricating a compact SoS AWG, the high refractive index contrast waveguides are used, such as 1.5%— Δ ^[3], 2.5%— Δ ^[4], and even extremely high refractive index contrast^[5], but spot-size converters or high-NA fibers are needed to reduce the high coupling losses to the standard single mode fibers. For the purpose to obtain the advantages of low refractive index contrast (i. e. low coupling losses to the standard single mode fibers) and higher refractive index contrast (i. e. compact size), a scheme by integrating a pair of air trenches along the waveguide bend to employ a high refractive index contrast was proposed^[6-7], and this scheme was used in fabricating the arrayed waveguides of AWGs in recent years^[8]. Although the size of AWG by using air trench (AT) bend waveguides in arrayed waveguides could be reduced greatly, but the performance, especially the

Foundation item: The National Key Technology R&D Program of China (No. 2009BAH49B02)

First author: WANG Wen-min(1975—), male, Ph. D. degree candidate, mainly focuses on optical components based on planar lightwave circuit. Email: wenmin.wang@accelink.com

Corresponding author: LIU Wen(1960—), male, professor, mainly focuses on optical components for optical communications. Email: liuwen@wri.com.cn

Received date: 2011-03-08 **Revised date:** 2011-04-29

crosstalk was lowered, for phase errors introduced by trenches. Furthermore, there were many literatures about optimizing the structure and performance of AWG domestically^[9-11], but there were few about the compact AWG.

In this paper, we propose a new scheme with inherent good performance which can reduce the size of low refractive index contrast AWG by only using air trench (AT) waveguides in parts of the input and output waveguides.

1 Design and discussion

The scheme of the new compact AWG is shown in Fig. 1. The structure of the proposed AWG has the characteristics as below.

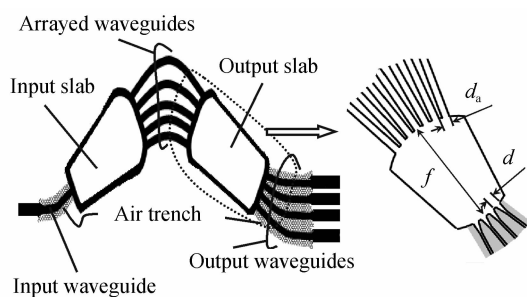


Fig. 1 Scheme of the compact AWG

In this AWG, both sides of the segments connected with slab waveguides in the input and output waveguides are trenched to form high refractive index contrast waveguides. The segments coupling to fibers in input or output waveguides and the arrayed waveguides are all fabricated with low refractive index contrast waveguides, for the purpose to obtain low coupling losses with fibers and good performances as traditional SoS AWGs.

The advantage of the AT waveguide is its high refractive index contrast, which is as large as $31\% - \Delta$, when the AWG is manufactured with a refractive index contrast of $0.75\% - \Delta$, so the widths of the AT waveguides and the gaps between them could be very small. For a SoS AWG made with refractive index contrast of $0.75\% - \Delta$, the space between the adjacent output waveguides is about $20 \sim 30 \mu\text{m}$ popularly. However, it can be as small as $4 \mu\text{m}$ for AT waveguides, which is mainly determined by the fabrication technology. The width of an AT waveguide can be as small as $2 \mu\text{m}$ ^[8], and the $2 \mu\text{m}$ gap between them is large enough to assure low coupling between them. For the space between the adjacent output waveguides can be much smaller than that of the traditional

AWG, the slab lengths and the numbers of the arrayed waveguides can be reduced greatly, and the AWG size can be reduced dramatically.

The scheme of the proposed AT input and output waveguides is shown in Fig. 2. As shown in Fig. 2, each of the AT output waveguides consists of a straight taper and a connection waveguide.

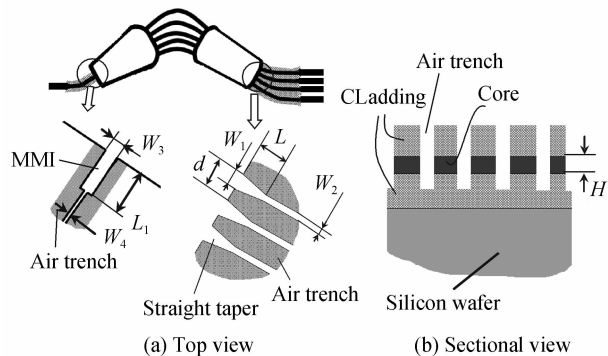


Fig. 2 Scheme of the input and output waveguides

The connection waveguide consists of AT straight waveguide(s) and bend waveguide(s) used to connect with the straight waveguide without AT. The taper's end width connected with output slab is W_1 , and the other end width is W_2 which equals the width of the connection waveguide. The taper length is L . The space between adjacent output waveguides connected with the output slab is d . There are many methods to realize flattened passband by using proper input waveguide structure^[12-13], and a multimode interference (MMI) waveguide is used as shown in Fig. 2. The width of the MMI is W_3 , and its length is L_1 . The MMI is connected with a connection waveguide with width of W_4 . Here, the width of $W_4 = W_2$. Both the W_4 and W_2 are chosen as $2 \mu\text{m}$, for the AT waveguide with width thinner than $2 \mu\text{m}$ is easily broken^[8]. By using proper L_1 , W_3 , and W_1 , we can realize an AWG with flattened passband. The refractive index of cladding is N_B , that of the core is N_C , and the height of the core is H . Here a refractive index contrast of $0.75\% - \Delta$ is used, where N_B is adopted as 1.4444, and H is $5.5 \mu\text{m}$. There are many literatures about fabrication and design technology of air trench^[6-8,14], and we will not discuss it in this paper. It should be noted here, the structure connecting the AT waveguide with the low refractive index contrast waveguide should be designed carefully to obtain low connection optical loss, and the detailed designs were discussed in many papers^[6-8,15], so we do not discuss it in this paper, too.

2 Example

We use the effective index method and finite-difference beam propagation method to simulate this AWG. We calculate band-width of the spectrum of the AWG under different W_3 . W_1 is decided by W_3 and the requirement of flatness of transmission spectrum. L_1 is selected to assure the phases difference between the 0 mode and 2nd mode is $(2k + 1)\pi$, where the integer $k \geq 0$. The simulated L_1 and W_1 under different W_3 are listed in Table 1. For the requirement of compactness, the gap between the output waveguides should be small enough, and the minimum gap between the output waveguides is $2 \mu\text{m}$ here, which is large enough to avoid coupling between the adjacent waveguides, so the space of d equals to $(W_1 + 2 \mu\text{m})$.

Table 1 Parameters of MMI and taper waveguide

MMI width, $W_3/\mu\text{m}$	MMI length, $L_1/\mu\text{m}$	Taper width, $W_1/\mu\text{m}$
4	337	2.7
5	344	3.65
6	332	4.4
7	343	5.25

Under different W_3 , the simulated relative passband width and peak loss of the transmission spectra for TE mode are shown in Fig. 3. The transmission spectra are shown in Fig. 4. In Fig. 3, the relative n dB-passband width is the ratio between the n dB-passband width and the channel spacing of AWG, where n equals 1 or 3. In Fig. 4, the relative wavelength is the ratio of the wavelength difference and the channel spacing, where the wavelength difference is the difference between the optical wavelength and the center wavelength of the spectrum. The center wavelength is 1550 nm for simulation. For a

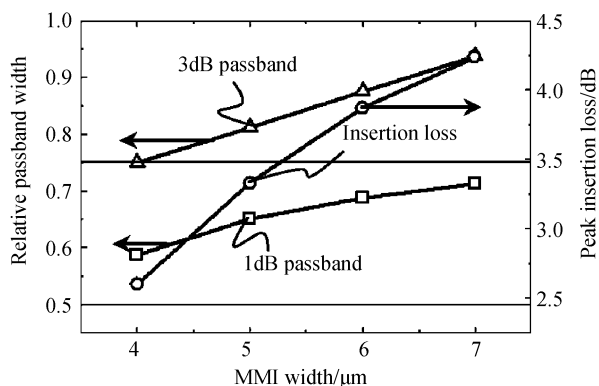


Fig. 3 Simulated 1 dB-passband, 3 dB-passband, and peak loss of the transmission spectra under different width of MMI waveguide

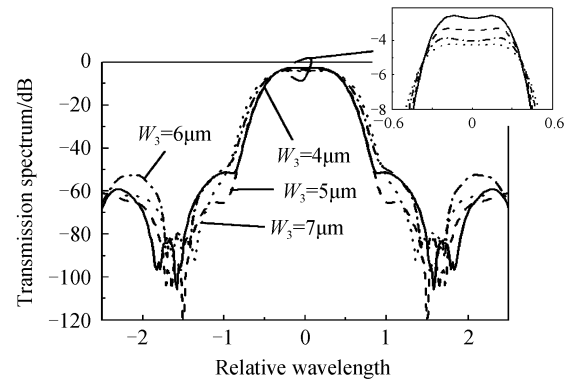


Fig. 4 Simulated transmission spectra of AWG flattened AWG-type demultiplexer, the relative 1 dB-passband and 3 dB-passband widths are required larger than 0.5 and 0.75, respectively. By compromising the passband width and the insertion loss, the proper MMI width should be about $5 \mu\text{m}$ according to Fig. 3 and 4.

When the MMI width is $5 \mu\text{m}$, the relative 1 dB-passband and 3 dB-passband width are 0.65 and 0.81, respectively, and the peak insertion loss is 3.3 dB for obtaining flattened passband. Furthermore, adjacent crosstalk is better than 44 dB as Fig. 4 shows, which is far better than a commercial requirement of 25 dB. Comparing with the traditional low refractive index contrast SoS AWG, the proposed AWG has better crosstalk, because much less optical field on the outside of the AT waveguides. When the width of MMI is $5 \mu\text{m}$, the space of d is $5.65 \mu\text{m}$, which is much smaller than that of traditional flattened SoS AWG designed with refractive index contrast of $0.75\% - \Delta$, so the size of the new AWG would be greatly reduced.

However, the structure of AT waveguide is asymmetric, so its TE mode index is different from the TM mode index. The difference between the TE and TM mode index of AT waveguides may introduce a big polarization dependent loss (PDL). For the purpose to evaluate the PDL caused by AT waveguides and optimize the AWG's structure to obtain good PDL, we simulate the relationship between the MMI length L_1 and the transmission loss when the relative wavelength equals 0, and the simulated results are shown in Fig. 5. As shown in Fig. 5, the dash-line curve indicates the relationship between the MMI length L_1 and the transmission loss for TE mode, and solid-line curve indicates that for TM mode. When the transmission loss locates on any pit of the dash-line curve, the AWG transmission spectrum for TE mode will be similar as that shown in Fig. 4. The

difference of transmission loss between the TE and TM mode is the PDL when the relative wavelength equals 0. From the Fig. 5, we can find the PDL will be as large as 1.4 dB, if LI equals $344 \mu\text{m}$. Fortunately, we can select proper size of MMI to realize low polarization dependent AWG. when L_1 equals $350 \mu\text{m}$, W3 equals $5.5 \mu\text{m}$, and W1 equals $3.65 \mu\text{m}$, the transmission losses for TE and TM mode are similar to each other near the center wavelength, and the transmission spectra for them are flattened. We simulate the AWG transmission spectra for TE and TM mode when L_1 equals $350 \mu\text{m}$ and W3 equals $5.5 \mu\text{m}$, and the simulated results are shown in Fig. 6. In Fig. 6, the dash-line curve indicates the transmission spectrum for TE mode, and the solid-line curve indicates that for TM mode. For the DWDM system, the PDL is popularly calculated in its clear pass-band. Popularly, the clear pass-band is defined as $\pm 12.5\%$ of the channel spacing around the center wavelength. For example, the clear pass-band is popularly $\pm 0.1 \text{ nm}$ around the center wavelength, when the channel spacing is 100 GHz (i. e. 0.8 nm). According to Fig. 6, the PDL introduced by AT waveguides will be smaller than 0.15 dB in

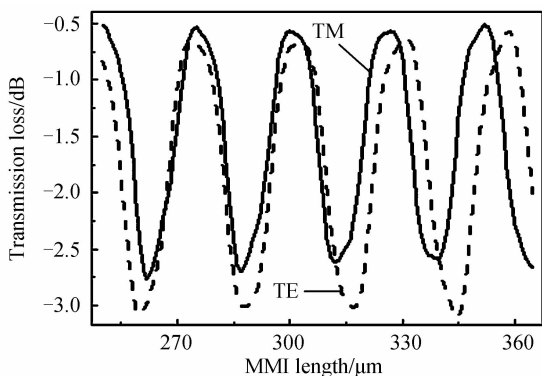


Fig. 5 Simulated transmission loss of AWG for TE and TM mode varied with MMI length when the relative wavelength equals 0

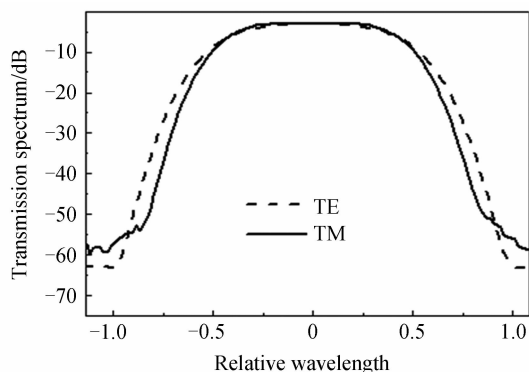


Fig. 6 Simulated transmission spectra of AWG for TE and TM mode when MMI length is $316 \mu\text{m}$ and W3 equals $5.5 \mu\text{m}$

the clear pass-band, which is far smaller than 0.5 dB required by the DWDM systems. The adjacent crosstalk for TE and TM mode are larger than 43 dB and 47 dB , respectively, and they are all better than the requirement of DWDM system.

For the purpose to show what the size of the new AWG should be, an AWG consisting 40 channels on 100 GHz ITU grid is designed.

To design an AWG, the focus of the slab waveguide f , the length difference between the adjacent waveguides ΔL , and the lateral spacing of the waveguides in the array aperture d_a should be determined firstly.

The focus f decides the insertion loss uniformity. The relationship between the insertion loss uniformity and f is [16]

$$L_U = -10 \log(e^{-2\theta_{\max}^2/\theta_0^2}) \quad (1)$$

where

$$\theta_{\max} = 20d/f \quad (2)$$

$$\theta_0 = \frac{\lambda_0}{N_{\text{FPR}} W_\epsilon} \frac{1}{\sqrt{2\pi}} \quad (3)$$

where N_{FPR} is the mode index in slab, which is 1.45233 here, and W_ϵ is the effective mode field width, which is about $3 \mu\text{m}$. λ_0 is the center wavelength of AWG, which is 1544.925 nm here. For meeting the requirement of insertion loss uniformity smaller than 0.5 dB , the length of f should be larger than $3350 \mu\text{m}$. Here f is set as $3500 \mu\text{m}$ to obtain better insertion loss uniformity.

Because $\Delta L = m\lambda_0/N_g$, where integer m is the phase array order, and N_g is the mode index of the arrayed waveguide, which is 1.44975 , so ΔL is decided by m . The dispersion D of the arrayed waveguide is decided by m and d_a as

$$D = \frac{\lambda_0}{f_c N_{\text{FPR}}} \frac{m}{d_a} \quad (4)$$

where f_c is the center frequency of AWG, which can be calculated from λ_0 by $f_c = c/\lambda_0 = 194049.846 \text{ GHz}$, and c is light speed in vacuum. D equals to $d/100 \text{ GHz}$. Thus the m/d_a equals $2.945 \mu\text{m}^{-1}$. We set m as 24, and the calculated d_a is $8.15 \mu\text{m}$. For the arrayed waveguide width is $5.5 \mu\text{m}$, it is large enough to assure there is at least $2 \mu\text{m}$ gap between the adjacent arrayed waveguides when d_a equals $8.15 \mu\text{m}$, where the SoS technology requires the minimum gap should be large enough to assure the cladding can be deposited completely (popularly, the minimum gap is about $2 \mu\text{m}$). Furthermore, the d_a is small enough to assure there is an enough coupling between the adjacent arrayed waveguides

near the slab waveguide to lower the AWG insertion loss. When m equals 24, the free spectrum range of the AWG is 8 085. 41 GHz, which is large enough to include 40 channels with 100 GHz spacing.

By using these parameters calculated above, we design a compact AWG. In this AWG, the number of arrayed waveguides is 351. The space between the ends of two adjacent output waveguides coupling with fibers is $127 \mu\text{m}$. The minimum bend radius in arrayed waveguides is $5\,007 \mu\text{m}$, and the minimum bend radius in AT waveguides is $300 \mu\text{m}$. The length and width of a single AWG are 23. 88 mm and 9. 7 mm, respectively as shown in Fig. 7(a), while the size of traditional $0.75\%-\Delta$ SoS AWG is larger than $40 \text{ mm} \times 30 \text{ mm}$. Forty-nine pieces of square AWG dies can be cut from a six inch silicon wafer as Fig. 7(b) shows.

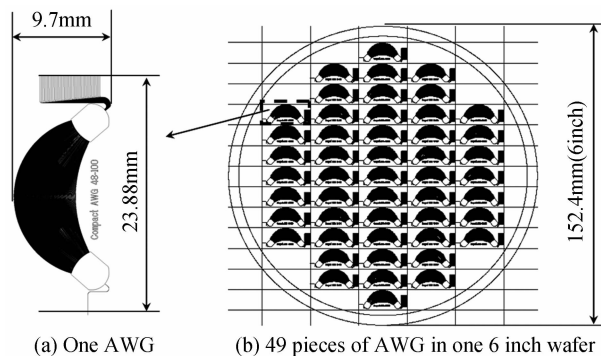


Fig. 7 Scheme of the layout of the compact AWG

3 Conclusion

From the discussions above, we can conclude that the compact size AWG can be obtained by etching air trenches on both sides of the segments in the input and output waveguides connected with the slab waveguides to form high refractive index contrast waveguides. For the segments of input and output waveguides coupling to the fibers are low refractive index contrast waveguides, the coupling losses with fibers can be small. The crosstalk and polarization dependent wavelength shift can be as same as a low refractive index contrast AWG, for the arrayed waveguides are the same as that of a low refractive index contrast AWG. The simulated results show an AWG consisting 40 channels on 100 GHz ITU grid can be as small as $23.88 \text{ mm} \times 9.7 \text{ mm}$ (the real AWG die is $23.88 \text{ mm} \times 10.5 \text{ mm}$), while its insertion loss uniformity, 1 dB-passband, and 3 dB pass band can be better than 0.5 dB, 0.52 nm, and 0.65 nm, respectively. The size of a traditional AWG with

the same function and material is about $43 \text{ mm} \times 35 \text{ mm}$, so the area of this compact AWG is about 1/6 of the traditional one.

The main drawback for the compact AWG introduced in this paper is that the air trenches are easily contaminated by dust, water, and impurities. The hermetic package can be used to protect the AWG chip from contamination. Further more, J. Ito and H. Tsuda suggested a method to protect the AWG chip by filling a low-refractive index material (CytotTM) into the trenches in 2009.

Although the design in this paper is an AWG consisting 40 channels, we can expand this design to one consisting more channels. For example, the size of a compact AWG consisting 192 channels on 25 GHz ITU grid is comparable with that of a traditional low refractive index contrast SoS AWG consisting 48 channels on 100 GHz ITU grid, because the space of adjacent output waveguides d of a traditional low refractive index contrast SoS AWG is about $25 \mu\text{m}$, which is at least 4 times of that of the compact AWG proposed in this paper.

References

- [1] BARBARIN Y, LEIJTENS X J M, BENTE E A J M, *et al.* Extremely small AWG demultiplexer fabricated on InP by using a double-etch process [C]. The Integrated Photonics Research (IPR), San Francisco, California, USA, 2004, Paper IThG4.
- [2] SMIT M K. Progress in AWG design and technology [C]. The Proceedings of 2005 IEEE/LEOS Workshop on Fibres and Optical Passive Components, Palermo, Italy, 2005, 26-31.
- [3] TAKADA K, ABE M, SHIBATA M, *et al.* Low-crosstalk 10 GHz-spaced 512-channel arrayed-waveguide grating multi/demultiplexer fabricated on a 4-in wafer [J]. *IEEE Photonics Technology Letters*, 2001, **13**: 1182-1184.
- [4] MARU K, OKAWA M, ABE Y, *et al.* Silica-based $2.5\%-\Delta$ arrayed waveguide grating using simple polarisation compensation method with core width adjustment [J]. *Electronics Letters*, 2007, **43**(1): 26-27.
- [5] KOHTOKU M. Low-loss compact silica-based AWG using deep ridge waveguide [C]. Presented at the Integrated Photonics Research and Applications, San Diego, California, USA, 2005, Paper ITuF1.
- [6] POPOVIC M, WADA K, AKIYAMA S, *et al.* Air trenches for sharp silica waveguide bends [J]. *Journal of Lightwave Technology*, 2002, **20**(9): 1762-1772.
- [7] AKIYAMA S, POPOVIC M A, RAKICH P T, *et al.* Air trench bends and splitters for dense optical integration in low index contrast [J]. *Journal of Lightwave Technology*, 2005, **23**(7): 2271-2277.
- [8] ITO J, TSUDA H. Small bend structures using trenches filled with low-refractive index material for miniaturizing silica planar lightwave circuits [J]. *Journal of Lightwave Technology*, 2009, **27**(6): 786-790.
- [9] LI De-lu, MA Chun-sheng, WANG Yu-hai, *et al.* Optimum design of polymeric arrayed waveguide grating with Fermi-like cross-section [J]. *Acta Photonica Sinica*, 2009, **38**(3): 541-

- 546.
- [10] LI De-lu, MA Chun-sheng, QIN Zheng-kun, *et al.* Parameter optimization of athermal arrayed waveguide grating using silica/polymer hybrid materials [J]. *Acta Photonica Sinica*, 2008, **37**(3): 369-472.
- [11] XU Ying-chao, ZHANG Guo-wei, E Shun-lin, *et al.* A new design to reduce insertion loss and crosstalk of AWG [J]. *Acta Photonica Sinica*, 2007, **36**(2): 224-228.
- [12] AMERSFOORT M R, SOOLE J B D, LEBLANC H P, *et al.* Passband broadening of integrated arrayed waveguide filters using multimode interference couplers [J]. *Electronics Letters*, 1996, **32**(5): 449-451.
- [13] WANG Wen-min, XU Yuan-zhong, MA Wei-dong, *et al.* DWDM based on AWG with wide pass-band and low crosstalk [C]. *SPIE*, 2004, **5279**: 611-617.
- [14] OU H, ROTTWITT K. Trenches for building blocks of advanced planar components [C]. *Optical Amplifiers and Their Applications*, San Francisco, California, USA, 2004, Paper JWB29.
- [15] FAN T Y T, ITO J, SUZUKI T, *et al.* Compact arrayed-waveguide grating using air trench and high mesa structure [C]. *Integrated Photonics Research and Applications (IPRA)*, Uncasville, Connecticut, USA, 2006, Paper IMB3.
- [16] SMIT M K, DAM C V. PHASAR-based WDM-devices: principles, design and applications [J]. *IEEE Journal of Selected Topics in Quantum Electronics*, 1996, **2**(2): 236-250.

小尺寸低折射率差硅基二氧化硅阵列波导光栅

王文敏^{1,2}, 刘文¹, 马卫东²

(1 华中科技大学 武汉光电国家实验室, 武汉 430074)

(2 武汉光迅科技股份有限公司, 武汉 430074)

摘要:随着阵列波导光栅(Arrayed Waveguide Grating, AWG)型器件在光通信系统中的大规模应用,对低成本 AWG 芯片的需求越来越多.在各种降成本方案中,减小 AWG 芯片的尺寸是最有效的方法之一.本文介绍了一种新型小尺寸低折射率差硅基二氧化硅 AWG 的设计.在该 AWG 中,输入波导/输出波导与平板波导连接的部分制作成两侧为空气槽的高折射率差波导,所以在与输出平板波导连接处的相邻输出波导间距较小,这样可以在设计上缩短平板波导的长度、减少阵列波导的数量,实现较小的 AWG 芯片尺寸.该 AWG 的其它部分,如输入/输出波导与光纤耦合的部分、阵列波导光栅等均采用常规的低折射率波导工艺,所以就同时具有与常规的低折射率波导 AWG 相同的优点:如低耦合损耗、较好的串扰以及光学特性等.根据这个原理,设计了一种 40 通道 100 GHz 频率间隔的低折射率差硅基二氧化硅 AWG,其芯片尺寸只有 23.88 mm×10.5 mm,是传统相同材料制作的 AWG 尺寸的 1/6.

关键词:空气槽;阵列波导光栅;通带宽度;硅基二氧化硅技术